Published in final edited form as:
Ophthalmology. 2005 February ; 112(2): 238–244.

Anterior Chamber Width Measurement by High-Speed Optical Coherence Tomography

Jason A. Goldsmith, MD, MS[1], **Yan Li, MS**[1,2], **Maria Regina Chalita, MD**[1], **Volker Westphal, PhD**[2], **Chetan A. Patil, BS**[2], **Andrew M. Rollins, PhD**[2,3], **Joseph A. Izatt, PhD**[4], and **David Huang, MD, PhD**[1,2,5]

1*Cole Eye Institute, Cleveland Clinic Foundation, Cleveland, Ohio.*

2*Department of Biomedical Engineering, Case Western Reserve University, Cleveland, Ohio.*

3*Department of Medicine, Case Western Reserve University, Cleveland, Ohio.*

4*Department of Biomedical Engineering, Duke University, Durham, North Carolina.*

5*Department of Biomedical Engineering, Lerner Research Institute, Cleveland Clinic Foundation, Cleveland, Ohio.*

Abstract

Objective: To measure anterior chamber (AC) width and other dimensions relevant to the sizing of phakic intraocular lenses (IOLs) with a high-speed optical coherence tomography (OCT) system.

Design: Cross-sectional observational study.

Participants: Both eyes of 20 normal volunteers.

Methods: A novel high-speed (4000 axial scans/second) OCT prototype was developed for anterior segment scanning. The system uses long wavelength (1310 nm) for deeper angle penetration, rectangular scanning for undistorted imaging, and short image acquisition time (0.125 seconds) to reduce motion error. Three horizontal cross-sectional OCT images (15.5 mm wide and 6 mm deep) of the anterior segment were obtained from each eye with real-time image display to guide centration on the corneal apex. Image processing software was developed to correct for image warping resulting from index transitions. Anterior chamber dimensions were measured using computer calipers by 3 expert raters (ophthalmologists). Analysis of variance was used to determine interrater, interimage, right versus left eye, and intersubject standard deviation (SD) of OCT measurements.

Main Outcome Measures: Anterior chamber width (recess to recess), AC depth, and crystalline lens vault as measured by OCT; external white-to-white (WTW) corneal diameter (CD) as measured by Holladay-Godwin gauge.

Results: The mean AC width was 12.53±0.47 mm (intereye SD), and the mean corneal diameter was 11.78±0.57 mm. Optical coherence tomography measurement of AC width has good repeatability from image to image (SD, 0.134 mm), but there was significant difference between raters (SD, 0.215 mm). Estimation of AC width from WTW CD by linear regression was relatively inaccurate (residual SD, 0.41 mm). The mean AC depth was 2.99±0.323 mm (intereye SD), with

Correspondence to David Huang, MD, PhD, Doheny Eye Institute, 1450 San Pablo Street, DEI 5702, Los Angeles, CA 90033. E-mail: davidhuang@alum.mit.edu..

Poster presented at: American Academy of Ophthalmology Annual Meeting, October, 2002; Orlando, Florida.

Supported by the National Eye Institute, Bethesda, Maryland (grant no.: R24 EY13015).

Dr Huang has patent interest in the optical coherence tomography technology. Drs Huang and Li receive research grant support from Carl Zeiss Meditec, Inc., Dublin, California. The other authors have no proprietary interest related to this article's topic.

repeatability of less than 0.001 mm (interimage SD), and the mean crystalline lens vault was 0.39 ±0.27 mm with 0.023 mm repeatability.

Conclusions: Reproducible OCT AC biometry was demonstrated using a high-speed OCT prototype. Further improvement in reproducibility may be achieved by automating the measurements with a computer. Direct OCT AC width measurement may improve sizing of angle-supported AC IOLs over conventional estimation by WTW CD. The measurement of AC depth and lens vault also may be useful for other types of phakic AC IOLs.

Interest in the use of phakic intraocular lenses (IOLs) for the treatment of high myopia and hyperopia is increasing.[1] Several approaches have been advocated, including irisfixated anterior chamber (AC) phakic IOLs,[2,3] posterior chamber phakic IOLs,[4] and angle-supported phakic IOLs.[5,6] This study focuses on the use of corneal and anterior segment (CAS) optical coherence tomography (OCT) as a biometric instrument for the measurement of AC parameters. The intended future application is for accurate sizing of angle-supported phakic IOLs.

For low to moderate myopia and hyperopia, excimer laser refractive surgery currently is the accepted procedure of choice. However, for eyes with high ametropia, laser ablation of the cornea is less attractive because of the risks of induced ectasia and aberrations. Clear lens extraction is an alternative, but the loss of accommodation and the risk for retinal detachment are serious concerns in many cases. The placement of a phakic IOL has the benefit of retaining accommodation. Of the various styles of phakic IOL, angle supported phakic IOLs offer ease of implantation (relative to iris-fixation IOLs) and less risk of cataract induction (compared with phakic posterior chamber IOLs). Excellent refractive outcomes for the treatment of high myopia have been demonstrated.[7,8] However, angle-supported phakic IOLs have been associated with several potential complications,[1] many of which arise from poor sizing. Pupil ovalization, iris atrophy, and iritis[9] occurs when the IOL is too large, causing excessive pressure on the iris root and angle recess by the haptic footplates. Undersized IOLs may become mobile and may result in endothelial damage, iritis, peripheral anterior synechiae, and secondary glaucoma.[10,11]

To reduce the incidence of these complications, accurate AC biometry is necessary. With a properly sized angle-supported AC IOL, the haptics sit on the scleral spur[9,10] or gently within the angle recess,[12] and the IOL vault places it approximately midway between the iris and cornea. Traditionally, external white-to-white (WTW) corneal diameter (CD) measurement has served as a surrogate for AC width,[9,13] because no practical means of internal AC width determination was available. Measurement of the external corneal diameter, however, depends on external limbal landmarks that may not correlate well with internal landmarks (e.g., scleral spur and angle recess). External measurement also can be biased significantly by pannus, arcus senilis, and other anatomic variations.

We believe that OCT is a promising method for accurate anterior segment biometry because of its high spatial resolution and noncontact nature.[14] However, technological development is needed to adapt OCT for this purpose. Several investigators have reported on the application of the commercially available OCT retinal scanners such as the OCT1/2 by Carl Zeiss Meditec, Inc. (Dublin, CA) for anterior segment analysis, including imaging of the cornea[15] and nonpenetrating glaucoma filtration sites.[16] The retinal scanner is limited by low speed (1 second per image), low transverse sampling (100 axial scans/image), and narrow depth of scan (approximately 2 mm in air). The sector scan geometry (expanding fan) of the retinal scanner when applied to the anterior segment makes accurate width measurement impossible. Furthermore, the 0.8-μm wavelength used for retinal scanning cannot penetrate the sclera to visualize angle structures such as the scleral spur and angle recess.[17]

We have developed a CAS OCT system that overcame these limitations. This CAS OCT system uses a longer wavelength (1.3 μm), allowing greater penetration through highly scattering tissues such as limbus and sclera, thus yielding visualization of angle structures. Furthermore, because the ocular media absorb approximately 90% of 1.3-μm light before it can reach the retina, higher power can be used safely, allowing near video-rate imaging. This system was used previously to demonstrate corneal and anterior segment imaging in a sector scan geometry.[18]

For this study, we further improved the CAS OCT system by using a wide-field rectangular scanning geometry to reduce image distortion.[19] Real-time video and OCT display and a slit-lamp base were added to improve alignment. The improved prototype was tested for reproducibility of AC biometry in this study.

Subjects and Methods

The study design and procedures were approved by the Institutional Review Board of the Cleveland Clinic Foundation. The study was compliant with the Health Insurance Portability and Accountability Act of 1996. Twenty volunteers, age 18 or older and without history of ocular disease, were recruited from the employees of the Department of Ophthalmology at the Cleveland Clinic. Anterior segment examination by slit lamp confirmed the normal status of the eyes. Informed consent was obtained from all volunteers.

Both eyes of each subject were measured with the experimental CAS OCT system. The CAS OCT prototype uses an infrared superluminescence diode light source at a wavelength of 1310 nm (OptoSpeed, Mezzovico, Switzerland), a coherence length of 40 nm. The OCT beam energy delivered to the eye was measured to be 2.5 mW. The system performs 4000 axial scans per second. For this study, each OCT cross-sectional image consisted of 500 axial scans. Thus, the acquisition time for each image was 0.125 milliseconds. The OCT images were displayed continuously at 8 frames per second, along with a video image displayed at 60 frames per second. The scanner was designed to provide a rectangular cross-sectional scan for minimal image distortion and accurate transverse dimension measurement. We set the image dimensions to be 15.5 mm wide and 6.0 mm deep (in air). The axial resolution was 19 μm full-width-half-maximum in tissue (25 μm in air), and the transverse resolution was 54 μm (beam diameter at focus). Subjects were asked to fixate on a distant, wall-mounted target with the contralateral eye to maintain straight-ahead gaze. Spectacles or contact lenses, if worn, were removed before OCT scanning. Imaging was made in normal room lighting. Three horizontal cross-sectional scans were obtained sequentially by a trained ophthalmic technician. The cross sections were centered on the corneal apex reflection. The corneal apex is identified easily on the realtime OCT images by its strong anterior surface reflection.

We developed image processing software using MatLab (Mathworks Inc., Natick, MA). The software compensates for index of refraction transitions at the air-tear interface and the different group indices in air, cornea, and aqueous to correct the physical dimensions of the images. The corrected images are displayed on a computer screen for computer-aided biometric measurements by expert raters.

Three ophthalmologists (JAG, MRC, DH) served as expert raters and independently measured the AC dimensions using computer caliper tools. Each image was displayed on a computer screen, and the angle recesses on both sides of the cross-sectional scan were marked on the screen by each rater. The recess-to-recess distance was recorded by the computer. The rater then identified the posterior corneal surface and the anterior crystalline lens surface along the anteroposterior (AP) axis perpendicular to the apex. On the OCT images, this AP axis is visualized as a flare extending from strong anterior corneal apex reflection. The computer then recorded the AC depth as the AP distance from the corneal endothelium to the lens surface.

The crystalline lens vault was measured as the AP distance between the anterior lens surface and the recess-to-recess line.

External white-to-white (WTW) corneal diameter (CD) was measured along the horizontal meridian in each eye of each subject using a Holladay-Godwin cornea gauge. The gauge is a hexagonal disk with calibrated semicircles marked on each side. The semi-circles have diameters between 9.0 and 14.0 mm in 0.5-mm increments. The gauge was held next to the examined eye so that its edges bisected the cornea horizontally as viewed by the examiner. To avoid parallax errors, the corneal ruler was held close to the eye being measured, and the rater closed his nondominant eye. Corneal diameter was determined by finding the semicircle that best approximated the corneal horizontal diameter. Two ophthalmic technicians were trained in this technique and independently made these measurements. Corneal diameter was measured once per rater.

All statistical analyses were performed using SAS.[20] Analysis of variance was used to determine interrater, interimage, right versus left eye, and intersubject standard deviation (SD) of OCT measurements.

Results

The CAS OCT prototype is shown in Figure 1. A wide-field horizontal cross-sectional image of the anterior segment generated using this device is shown in Figure 2. The 3 parameters measured in this study are illustrated in the figure. A close-up of the angle is shown in Figure 3. Both the scleral spur and the angle recess are visible in the OCT image. We chose to measure the AC width from recess to recess because this would be more relevant to the locations of the haptic footplates for an angle-supported IOL.

Participant Background Statistics

There were 13 female (65%) and 7 male (35%) subjects. Fifteen subjects (75%) were white, 3 (15%) were Asian, and 2 (10%) were black. On the basis of spherical equivalence, 16 subjects (80%) were bilateral myopes, 2 (10%) were bilateral hyperopes, 1 (5%) was bilaterally emmetropic, and 1 (5%) was a split myopic individual and hyperope.

Population Statistics of Biometric Parameters

The AC biometry results are summarized in Table 1 on an eye-by-eye basis. The average of measurements on each eye were used to calculate these population statistics. The intereye SD was equivalent to the root-mean-square sum of the intersubject and right versus left eye SD shown later.

Anterior Chamber Width versus Corneal Diameter

We compared the relationship between AC width and WTW CD using 2 models. The average of measurements on each eye was used.

The simpler model was similar to the conventional rules for sizing an AC IOL, where a constant is added to the WTW CD to obtain the IOL length. To estimate the constant offset between AC width and WTW CD, we calculated the difference and analyzed the statistical distribution. The mean difference was 0.748±0.439 mm (intereye SD), with a range of -0.314 to 1.843 mm.

The more sophisticated 2-parameter model used linear regression. A plot of AC width versus WTW CD is shown in Figure 4. Linear regression analysis generated the best-fit line shown in the figure. The root-mean-square residual (SD) for this model is 0.410 mm.

Anterior Chamber Width Analysis of Variance

As shown in Table 2, the largest component of variance in AC width measurement (67.96%) was the result of variability in AC width among the 20 subjects (intersubject variance). The right and left eyes were highly correlated within a subject. The second largest variance component (15.42%) was the result of systematic differences between the raters (interrater trend). Variability between the 3 OCT images obtained from each eye accounted for a relatively small component of the variance (6.03%). This interimage SD (0.134 mm) best represents the intrinsic variability of the OCT measurement.

Corneal Diameter Analysis of Variance

As shown in Table 3, the largest component of variation in corneal diameter was the result of variability in corneal diameter among the 20 subjects. There is relatively little difference between the left and right eyes. The differences between the 3 raters were primarily random rather than systematic.

Anterior Chamber Depth Variance

As shown in Table 4, the largest component of variance in AC depth was the result of variability in AC depth between the 20subjects. Variability between left and right eyes and between raters was very small. The difference between OCT images was not measurable (SD = 0).

Crystalline Lens Vault Variance

As shown in Table 5, the largest component of variance in crystalline lens vault was the result of variability between the 20 subjects. Variability between left and right eyes and between raters was small. The interimage variability was very small (SD = 23 μm).

Discussion

We believe this article is the first to describe OCT measurement of AC width and to assess its reproducibility. We were unable to find any previous report of this in the literature. The reproducibility from image to image was good (SD = 0.134 mm, or coefficient of variation of 1%). However, when combined with the variability between raters, the total SD goes up to 0.298 mm, which is only fair. Most of the difference between raters was systematic, with 1 rater generally measuring AC width approximately 0.3 to 0.4 mm smaller than that of the other 2 raters. The difference was the result of the identification of the apex of the angle recess, which can be ambiguous because of relatively low signal from the irisciliary body junction and speckle noise in the images. The identification of the recess apex could be enhanced by manipulating the image contrast and brightness. However, we have found the best solution to be a computer program that automatically locates the recess apices on both side of the AC without any human operator input. We have developed such software after this study and its performance will be published separately.

Because there is no noninvasive gold standard for AC width measurement, we were unable to assess the accuracy of our OCT measurements. However, our results agree well with a set of intraoperative measurements (Piovella M, et al. Correction of high myopia with foldable anterior chamber phakic IOL. Poster no. 262 at AAO Annual Meeting, November, 2002; Orlando, Florida). Piovella et al found a mean WTW CD of 11.7±0.4 mm, and an AC width as measured by the use of an intraoperative surgical sizer of 12.4±0.3 mm. In our study, the WTW CD was 11.78± 0.57 mm, and the AC width was 12.53±0.47 mm. Our eyes were slightly larger, possibly because of the prevalence of myopes in our study population.

Ultrasound imaging[21] is another method that could visualize the entire cross section of the AC from angle to angle. For example, the Artemis 2 (Ultralink LLC, St. Petersburg, FL) ultra-high-

frequency ultrasound system shows such images (www.arcscan.com). However, we were unable to find a systematic study of AC width using ultrasound imaging for comparison. A potential disadvantage of ultra-sound imaging is the need to immerse the eye in fluid with an eye cup or other holding device. The physical contact is more cumbersome and uncomfortable and may distort the shape of the eye. Optical coherence tomography does not have this limitation. However, ultrasound imaging has the advantage of better penetration and visualization of the posterior chamber. We are able to visualize the entire thickness of the iris with our OCT prototype, but visualization of the retro-iris lens, ciliary body, and ciliary sulcus is poor (Figs 2, 3).

Traditionally, the sizing of angle-supported AC IOLs is based on measuring the corneal diameter and adding a constant, such as 1 mm. A recent study showed that both manual measurements (Holladay-Godwin gauge, surgical caliper) and automated measurements (Orbscan II, Bausch & Lomb, Rochester, NY; IOL-Master, Carl Zeiss Meditec) provide comparable average values, but the automated instruments were more reproducible and less operator dependent. Unfortunately, we did not have an automated instrument for corneal diameter measurement in this study. However, in this study, we found that the main problem with using the WTW CD was not poor reproducibility (combined interrater SD = 0.29), but a lack of correlation between WTW CD and AC width. The difference between WTW CD and AC width had an SD of 0.44 mm, whereas the intereye SD of AC width was 0.47 mm. Even with the linear regression model, estimation of the AC width from the WTW CD had an SD of 0.41 mm. Thus, using the WTW CD information could improve the estimation of AC width only minimally compared with using the average value. This may explain the high incidence of sizing-related complications, such as pupil ovalization (iris retraction) and IOL movement and inflammatory response, in the treatment of high myopia with angle-supported IOLs.[6,7]

To demonstrate the potential for clinical improvement with better measurements, we calculated the misfit probability for angle-supported AC IOLs using the various sizing approaches (Table 6). The tolerance for fitting is assumed to be ±0.5 mm, the usual sizing increment for AC IOLs. Data from this study provide the SD estimates. The one-size-fits-all approach yields a 29% chance of the IOL being too large or small by 0.5 mm. Using WTW CD and a linear regression model to estimate the AC width only slightly improves the misfit probability to 22%. Using OCT and a human grader to measure the AC width manually with a computer caliper, the misfit probability improves to 9%. If we remove the subjective error of the manual caliper step and use completely automated computer image processing to locate the angle recesses and measure the AC width, the misfit probability is estimated to be 0.02%! This extremely low error rate is the result of the sizing tolerance being more than 6 times wider than the SD (commonly represented by σ or sigma) of OCT measurements. The improvement conforms to the Six Sigma goal commonly referred to in the total quality management literature. However, our calculations assume that OCT measurements do not contain significant systematic error. This assumption needs to be validated clinically. We suggest that future studies of phakic IOL implants include direct measurement of AC dimensions by either OCT or ultrasound to determine if these instruments may help in proper patient selection and IOL sizing and may reduce complications.

Corneal and anterior segment OCT cannot penetrate into the posterior chamber to measure the diameter of the ciliary sulcus ring. But even if the ciliary sulcus ring could be visualized directly, it has a complex geometry and varies significantly with accommodation, making it difficult to characterize with a single diameter value. The AC width may be a good surrogate parameter that is more stable than direct measurement of the sulcus ring diameter. Thus, CAS OCT also may have the potential to improve sulcus-supported phakic IOL sizing.

There are already multiple instruments that can measure the AC depth precisely. These include ultrasound A scan and B scan, slit scanning, Scheimpflug photography, and laser interferometry.[22-31] This study shows that OCT also is able to make this measurement very precisely. The interimage and interrater SD were 0, which means that the variation is less than our pixel depth (8.8 μm in aqueous). This value is important for estimating the clearance distance between an IOL and the cornea. We also found that OCT could measure the vault of the crystalline lens precisely relative to the angle recesses. We could not find a comparable value in the literature. However, this value may be useful in designing or fitting the optimal vault of an angle-supported IOL. Similarly, the OCT images could be used to predict the vault of an iris-fixated IOL. We did not study the lens-iris vault measurement here, because the relevant measurement landmarks depend on the specific IOL dimensions, of which we do not have knowledge.

We continue to improve the instrument and method to make OCT useful for AC biometry. The CAS OCT proto-type used in this study has the following features that are essential for precise measurement of AC width:

1. Sufficient penetration to visualize angle recess. This was achieved by using the 1.3-μm wavelength, which is longer than the 0.8-μm wavelength previously used for ocular OCT.
2. High speed to reduce motion artifact (8 image frames per second).
3. Rectangular scanning geometry to reduce image distortion.
4. Wide-field scanning optics (15.5 mm) and deep axial scan range (6 mm) to cover the entire AC in 1 image frame.
5. Image processing (dewarping software) to correct image distortion resulting from index transitions.

Based on the experience learned in this study, we believe the following improvements will enhance the accuracy of OCT biometry further:

1. Completely automated software for biometric measurements to remove human error.
2. Averaging of several image frames to reduce speckle noise.
3. Internal fixation target to better establish gaze direction during imaging.
4. Control of accommodation with the internal fixation target.

We believe that with these additional features, high-speed CAS OCT will become an accurate, dependable, and versatile tool for AC biometry and measurements of the cornea and anterior segment in general.

References

1. O'Brien TP, Awwad ST. Phakic intraocular lenses and refractory lensectomy for myopia. Curr Opin Ophthalmol 2002;13:264–70. [PubMed: 12165713]
2. Budo C, Hessloehl JC, Izak M, et al. Multicenter study of the Artisan phakic intraocular lens. J Cataract Refract Surg 2000;26:1163–71. [PubMed: 11008043]
3. Menezo JL, Cisneros AL, Rodriguez-Salvador V. Endothelial study of iris-claw phakic lens: four year follow-up. J Cataract Refract Surg 1998;24:1039–49. [PubMed: 9719962]
4. Arne JL, Lesueur LC. Phakic posterior chamber lenses for high myopia: functional and anatomical outcomes. J Cataract Refract Surg 2000;26:369–74. [PubMed: 10713231]
5. Alio JL, de la Hoz F, Ruiz-Moreno JM, Salem TF. Cataract surgery in highly myopic eyes corrected by phakic anterior chamber angle-supported lenses. J Cataract Refract Surg 2000;26:1303–11. [PubMed: 11020614]

6. Perez-Santonja JJ, Alio JL, Jimenez-Alfaro I, Zato MA. Surgical correction of severe myopia with an angle-supported phakic intraocular lens. J Cataract Refract Surg 2000;26:1288–302. [PubMed: 11020613]
7. Allemann N, Chamon W, Tanaka HM, et al. Myopic angle-supported intraocular lenses: two-year follow-up. Ophthalmology 2000;107:1549–54. [PubMed: 10919906]
8. Baikoff G, Arne JL, Bokobza Y, et al. Angle-fixated anterior chamber phakic intraocular lens for myopia of -7 to -19 diopters. J Refract Surg 1998;14:282–93. [PubMed: 9641419]
9. Saragoussi JJ, Othenin-Girard P, Pouliquen YJ. Ocular damage after implantation of oversized minus power anterior chamber intraocular lenses in myopic phakic eyes: case reports. Refract Corneal Surg 1993;9:105–9. [PubMed: 8494809]
10. Stamper, RL.; Sugar, A.; Ripkin, DJ. Intraocular Lenses: Basics and Clinical Applications. American Academy of Ophthalmology; San Francisco: 1993. p. 29-61.
11. Apple DJ, Mamalis N, Loftfield K, et al. Complications of intraocular lenses. A historical and histopathological review. Surv Ophthalmol 1984;29:1–54. [PubMed: 6390763]
12. Apple DJ, Brems RN, Park RB, et al. Anterior chamber lenses. Part I: complications and pathology and a review of designs. J Cataract Refract Surg 1987;13:157–74. [PubMed: 3572772]
13. Karickhoff JR. Instruments and techniques for anterior chamber implants. Arch Ophthalmol 1980;98:1265–7. [PubMed: 7396781]
14. Huang D, Swanson EA, Lin CP, et al. Optical coherence tomography. Science 1991;254:1178–81. [PubMed: 1957169]
15. Maldonado MJ, Ruiz-Oblitas L, Munuera JM, et al. Optical coherence tomography evaluation of the corneal cap and stromal bed features after laser in situ keratomileusis for high myopia and astigmatism. Ophthalmology 2000;107:81–7. [PubMed: 10647724]discussion 88
16. Nozaki M, Kimura H, Kojima M, Ogura Y. Optical coherence tomographic findings of the anterior segment after nonpenetrating deep sclerectomy. Am J Ophthalmol 2002;133:837–9. [PubMed: 12036684]
17. Izatt JA, Hee MR, Swanson EA, et al. Micrometer-scale resolution imaging of the anterior eye in vivo with optical coherence tomography. Arch Ophthalmol 1994;112:1584–9. [PubMed: 7993214]
18. Radhakrishnan S, Rollins AM, Roth JE, et al. Real-time optical coherence tomography of the anterior segment at 1310 nm. Arch Ophthalmol 2001;119:1179–85. [PubMed: 11483086]
19. Huang D, Li Y, Radhakrishnan S. Optical coherence tomography of the anterior segment of the eye. Ophthalmol Clin North Am 2004;17:1–6. [PubMed: 15102509]
20. SAS [computer program]. Version 8. SAS Institute; Cary, NC: 2001.
21. Pavlin CJ, Harasiewicz K, Sherar MD, Foster FS. Clinical use of ultrasound biomicroscopy. Ophthalmology 1991;98:287–95. [PubMed: 2023747]
22. Reddy AR, Pande MV, Finn P, El-Gogary H. Comparative estimation of anterior chamber depth by ultrasonography, Orbscan II, and IOLMaster. J Cataract Refract Surg 2004;30:1268–71. [PubMed: 15177602]
23. Goel S, Chua C, Butcher M, et al. Laser vs ultrasound biometry: a study of intra- and interobserver variability. Eye 2004;18:514–8. [PubMed: 15131684]
24. Rabsilber TM, Becker KA, Frisch IB, Auffarth GU. Anterior chamber depth in relation to refractive status measured with the Orbscan II Topography System. J Cataract Refract Surg 2003;29:2115–21. [PubMed: 14670419]
25. Sasaki H, Sakamoto Y, Harada S, et al. Predicting postoperative anterior chamber depth in cataract patients using Scheimpflug slit photography. Ophthalmic Res 2002;34:265–72. [PubMed: 12381886]
26. Sheng H, Bottjer CA, Bullimore MA. Ocular component measurement using the Zeiss IOLMaster. Optom Vis Sci 2004;81:27–34. [PubMed: 14747758]
27. Kurtz D, Manny R, Hussein M. COMET Study Group. Variability of the ocular component measurements in children using A-scan ultrasonography. Optom Vis Sci 2004;81:35–43. [PubMed: 14747759]
28. Tong L, Wong EH, Chan YH, Balakrishnan V. Agreement between Scheimpflug photography and A-scan ultrasonography in anterior segment ocular measurements in children. Optom Vis Sci 2003;80:529–34. [PubMed: 12858088]

29. Friedman DS, Gazzard G, Foster P, et al. Ultrasonographic biomicroscopy, Scheimpflug photography, and novel provocative tests in contralateral eyes of Chinese patients initially seen with acute angle closure. Arch Ophthalmol 2003;121:633–42. [PubMed: 12742840]

30. Kriechbaum K, Findl O, Kiss B, et al. Comparison of anterior chamber depth measurement methods in phakic and pseudophakic eyes. J Cataract Refract Surg 2003;29:89–94. [PubMed: 12551673]

31. Nemeth J, Fekete O, Pesztenlehrer N. Optical and ultrasound measurement of axial length and anterior chamber depth for intraocular lens power calculation. J Cataract Refract Surg 2003;29:85–8. [PubMed: 12551672]

Figure 1.
One of the authors (MRC) demonstrating the use of the corneal and anterior segment optical coherence tomography (OCT) prototype. The OCT hardware is contained within the black box on top of the slit lamp. The OCT image is displayed on the monitor on the right, and the charge-coupled device video is on the monitor on the left.

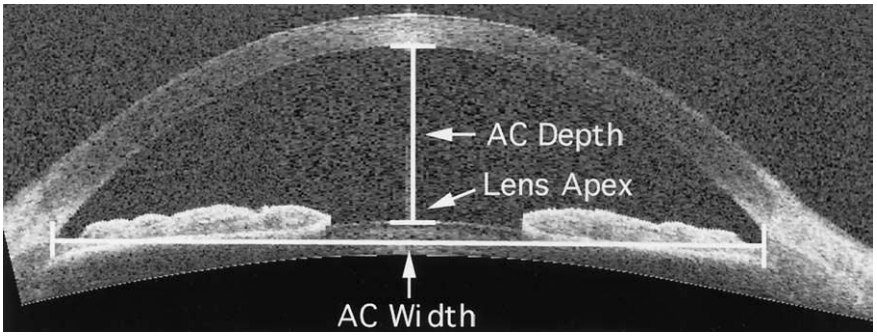

Figure 2.
Horizontal optical coherence tomography section of the anterior segment after computational correction for index transitions. The anterior chamber (AC) width is measured angle recesses. Anterior chamber depth is the anteroposterior (AP) distance from the corneal endothelium to the lens apex. Lens vault (not drawn) is the AP distance between the lens apex and the recess-to-recess line.

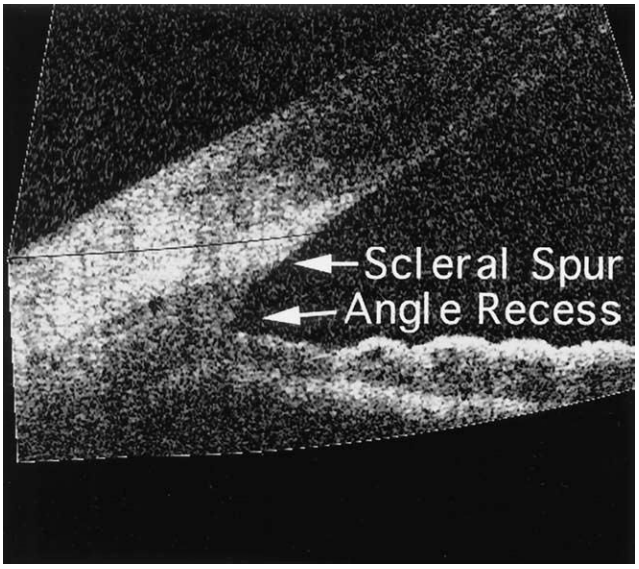

Figure 3.
Optical coherence tomography image of the iridocorneal angle demonstrating the scleral spur and angle recess.

Figure 4.
Plot of the optical coherence tomography (OCT) anterior chamber width versus white-to-white corneal diameter by eye. Each point is the average of measurements obtained from each eye. The linear regression line and equation are shown.

Table 1

Population Statistics for Anterior chamber Measurements

	Mean (mm)	Intereye Standard Deviation (mm)	Range (mm)
AC width*	12.53	0.47	11.48-13.54
Corneal diameter†	11.78	0.57	10.83-12.83
AC depth*	2.99	0.32	2.34-3.50
Crystalline lens vault*	0.39	0.27	-0.16-0.97

AC = anterior chamber.

* Measured by optical coherence tomography

† Measured by Holladay-Godwin gauge.

Table 2

Anterior Chamber Width Variance Components

Variance Components	Variance (mm^2)	% Variance	Standard Deviation (mm)
Intersubject	0.2037	67.96	0.451
Eye (right vs. left)	0.0073	2.45	0.086
Interrater trend	0.0462	15.42	0.215
Interrater random	0.0244	8.15	0.156
Interimage	0.0181	6.03	0.134

Table 3

Corneal Diameter Variance Components

Variance Components	Variance (mm^2)	% Variance	Standard Deviation (mm)
Intersubject	0.3034	72.88	0.551
Eye (right vs. left)	0.0261	6.28	0.162
Interrater trend	0.0157	3.77	0.125
Interrater random	0.0710	17.06	0.267

Table 4

Anterior Chamber Depth Variance Components

Variance Components	Variance (mm^2)	% Variance	Standard Deviation (mm)
Intersubject	0.1041	95.54	0.323
Eye (right vs. left)	0.0027	2.45	0.052
Interrater random	0.0022	2.01	0.047
Interrater trend	0	0	0
Interimage	0	0	0

Table 5

Crystalline Lens Vault Variance Components

Variance Components	Variance	% Variance	Standard Deviation (mm)
Intersubject	0.0684	87.39	0.261
Eye (right vs. left)	0.0041	5.21	0.064
Interrater random	0.0038	4.85	0.062
Interrater trend	0.0015	1.88	0.038
Interimage	0.0005	0.67	0.023

Table 6

Estimated Probability of Anterior Chamber Intraocular Lens Misfit

Sizing Method	Standard Deviation (mm)	P Value Deviation > 0.5 mm
One size fits all	0.47	28.74%
WTW linear regression	0.41	22.26%
OCT manual	0.298	9.34%
OCT automated	0.134	0.02%

OCT = ocular coherence tomography; WTW = white-to-white corneal diameter.